JVI Journals.ASM.org

Differential Pathological and Immune Responses in Newly Weaned Ferrets Are Associated with a Mild Clinical Outcome of Pandemic 2009 H1N1 Infection

Stephen S. H. Huang,[a,b] David Banner,[a] Norbert Degousee,[g] Alberto J. Leon,[a,e] Louling Xu,[a] Stephane G. Paquette,[a,c] Thirumagal Kanagasabai,[a] Yuan Fang,[a,b,e] Salvatore Rubino,[h] Barry Rubin,[g] David J. Kelvin,[a,b,c,d,e,f] and Alyson A. Kelvin[d]

Division of Experimental Therapeutics, Toronto General Research Institute, University Health Network, Toronto, Ontario, Canada[a]; Department of Immunology, Faculty of Medicine, University of Toronto, Toronto, Ontario, Canada[b]; Institute of Medical Science, Faculty of Medicine, University of Toronto, Toronto, Ontario, Canada[c]; Immune Diagnostics & Research, Toronto, Ontario, Canada[d]; International Institute of Infection and Immunity, Shantou University Medical College, Shantou, Guangdong, China[e]; Department of Biomedical Sciences, University of Sassari, Sassari, Sardinia, Italy[f]; Division of Vascular Surgery, Peter Munk Cardiac Centre, Toronto General Research Institute, University Health Network, Toronto, Ontario, Canada[g]; and Center for Biotechnology Development and Biodiversity Research, University of Sassari, Sassari, Sardinia, Italy[h]

Young children are typically considered a high-risk group for disease associated with influenza virus infection. Interestingly, recent clinical reports suggested that young children were the smallest group of cases with severe pandemic 2009 H1N1 (H1N1pdm) influenza virus infection. Here we established a newly weaned ferret model for the investigation of H1N1pdm infection in young age groups compared to adults. We found that young ferrets had a significantly milder fever and less weight loss than adult ferrets, which paralleled the mild clinical symptoms in the younger humans. Although there was no significant difference in viral clearance, disease severity was associated with pulmonary pathology, where newly weaned ferrets had an earlier pathology improvement. We examined the immune responses associated with protection of the young age group during H1N1pdm infection. We found that interferon and regulatory interleukin-10 responses were more robust in the lungs of young ferrets. In contrast, myeloperoxidase and major histocompatibility complex responses were persistently higher in the adult lungs; as well, the numbers of inflammation-prone granulocytes were highly elevated in the adult peripheral blood. Importantly, we observed that H1N1pdm infection triggered formation of lung structures that resembled inducible bronchus-associated lymphoid tissues (iBALTs) in young ferrets which were associated with high levels of homeostatic chemokines CCL19 and CXCL13, but these were not seen in the adult ferrets with severe disease. These results may be extrapolated to a model of the mild disease seen in human children. Furthermore, these mechanistic analyses provide significant new insight into the developing immune system and effective strategies for intervention and vaccination against respiratory viruses.

The differential impact of influenza virus infection in individuals of various ages has been well documented since the first influenza pandemic of the 20th century (93). Young children are considered an influenza high-risk group due to the large number of young cases throughout the history of influenza (45–47, 50, 73, 75, 78, 79, 90, 93, 96). In North America, the number of hospitalized children due to seasonal influenza epidemics can be as high as over 10 hospitalizations per 1,000 children, and the consultation rate from influenza outpatients can reach 10 patients per 100 children (20, 75).

There are several reasons that a young individual can have increased susceptibility to respiratory diseases. Young children's lungs have not fully developed and easily succumb to respiratory infections. Moreover, it may take more than 36 months postpartum before an infant lung matures into a fully functional lung. Infection-induced lung tissue damage can obstruct the narrow immature airway and cause surfactant deficiency, leading to collapsed lung and asphyxia (1, 9, 16). Furthermore, other developmental problems, such as neurological and cardiopulmonary conditions, have also been suggested to contribute to severe influenza illness in younger children (2, 10, 33, 43, 60, 78). As well, healthy children who have no predisposing problems may also be susceptible to influenza virus infections due to insufficient immunological responses to the pathogens. In contrast to adults, the immune system in neonates has been shown to be T_h2 prone and highly regulated under the interleukin-10 (IL-10) and transforming growth factor β (TGF-β) response network (5, 14, 82, 100). Therefore, young children are often considered immunocompromised due to their rather profound regulatory immunomodulation network that may restrict an efficient host defense to clear respiratory infections. Interestingly, the development of ectopic lymphoid organs, such as inducible bronchus-associated lymphoid tissues (iBALTs), is observed more frequently in infants or young individuals, especially when pulmonary insults such as infections or inflammatory triggers have occurred (31, 91). However, in healthy human adults, persistent exposure to stimuli such as smoking and chronic pulmonary inflammatory diseases is thought to be required for iBALT formation (19, 91). The difference between the adult and pediatric immune systems is significant and must be considered in respect to the disease course.

Received 11 June 2012 **Accepted** 2 October 2012
Published ahead of print 10 October 2012
Address correspondence to David J. Kelvin, dkelvin@uhnresearch.ca.
Supplemental material for this article may be found at http://jvi.asm.org/.

doi:10.1128/JVI.01456-12
The authors have paid a fee to allow immediate free access to this article.

Similar to the seasonal influenza virus infections, the clinical attack rate in pediatrics was also prominent during pandemic influenza seasons, including that involving pandemic 2009 H1N1 (H1N1pdm) infection (3, 13, 37, 42, 43). During the spring and fall 2009 pandemic waves in North America, pediatric patients accounted for at least 30% to 40% of the total H1N1pdm hospital admissions (32, 78). Unexpectedly, recent clinical reports and case studies suggested that the clinical symptoms of the majority of H1N1pdm pediatric patients were mild to moderate (32, 45, 52, 78, 89, 98, 99). In addition, severe H1N1pdm cases (including those requiring admission to an intensive care unit and those involving fatalities) were more frequent in the older age groups. From April 2009 to April 2010 in North America, the cumulative H1N1pdm mortality rate for pediatric patients was three to five times less than that for adults and about three times less than the overall mortality rate (32, 78). Typically, severe illness or mortality as a result of H1N1pdm infection was attributed to acute respiratory distress syndromes (ARDSs) which resulted from influenza-induced lung tissue damage that impaired gas exchange and led to hypoxemia and death (24, 27, 35, 36, 55, 58, 71, 77). Patients with ARDSs are often observed to have severe inflammation and leukocyte infiltration in the lungs, which obstruct the airways and which are believed to be the cause of ARDSs.

Ferrets are a superlative animal model of influenza virus infection as they manifest typical clinical symptoms of influenza and display immune responses similar to those of humans without the need to further adapt the virus in the animals, as is typically done in mice in most influenza cases (35, 36, 49, 57, 60, 62, 71, 80). Age-dependent pathogenic factors, such as neonatal ferret lung development in association with influenza virus infections, have been studied and shown to have similarities to those in humans (7–9, 38, 65, 80, 84). Here we sought to investigate the differential immune responses due to age following influenza virus infections that may contribute to the diverse clinical outcomes seen in humans. Specifically, we examined the pathogenesis of H1N1pdm in newly weaned and adult ferrets and the disease signatures of both groups. Clinical symptoms, viral load, lung histopathology, antibody responses, and gene expression of various leukocyte markers, cytokines, and chemokines in both H1N1pdm-infected age groups were analyzed. Our findings are the first to describe an immunological clinical and pathological picture for a protective response to H1N1pdm influenza virus infection in young ferrets. Furthermore, the identified mechanisms provide insight for the development of future therapeutic and immunization strategies.

MATERIALS AND METHODS

Ethics statement. All work with animals was conducted in strict accordance with the Canadian Council of Animal Care (CCAC) guidelines. The University Health Network (UHN) has certification with the Animals for Research Act (permit numbers 0045 and 0085 of the Ontario Ministry of Agriculture, Food and Rural Affairs) and follows NIH guidelines (OLAW A5408-01). The animal use protocol was approved by the Animal Care Committee (ACC) of UHN. All infections and sample collections were performed under 5% isoflurane anesthesia, and all efforts were made to minimize suffering.

Influenza virus and animals. The H1N1pdm virus strain A/Mexico/4108/2009 (Mex/4108) was provided in chicken egg allantoic fluid by the Influenza Reagent Resource, Influenza Division, WHO Collaborating Center for Surveillance, Epidemiology and Control of Influenza, Centers for Disease Control and Prevention, Atlanta, GA. All virus work was performed in a biosafety level 2+ (BSL-2+) facility. Male ferrets 5 to 8 weeks old (newly weaned) and male ferrets 4 to 6 months old (adult) were bred in an on-site specific-pathogen-free ferret colony (University Health Network, Toronto, ON, Canada). Before infection, ferrets were shown to be seronegative for currently circulating influenza A and B virus strains by hemagglutination inhibition (HI) assay.

Infection and ferret monitoring. Maintenance and monitoring of ferrets upon infection followed the methods previously described (35). Briefly, prior to infection, ferrets were randomly selected and housed in pairs in cages contained in bioclean portable laminar-flow clean-room enclosures (Lab Products, Seaford, DE) in the BSL-2+ animal holding area. Baseline body temperature and weight were measured on days −1 and 0 for each animal. Temperatures were measured by using a subcutaneous implantable temperature transponder (BioMedic Data Systems, Inc., Seaford, DE). On the day of infection, each ferret was anesthetized and infected with 1 ml of Mex/4108 inoculum (0.5 ml in each nostril) at a dosage of 10^6 50% egg infectious doses (EID_{50}s). Clinical signs (body temperature, body weight, level of animal activity, and symptoms of nasal discharge and sneezing) were observed daily for 14 days postinfection (p.i.). Uninfected newly weaned ferrets were housed in a separate non-BSL-2$^+$ animal holding area to prevent influenza virus transmission from the infected groups. We examined animals at the same time each day for consistency. Nasal discharge recorded the color, prominence, and location of crusty nose, mucous, and transparent exudates/fluids. The scores were calculated from the total number of animals displaying any nasal discharge symptom over the total number of animals. The sneezing scores were calculated from the total number of animals witnessed sneezing over the total number of animals. Scores were calculated daily for 14 days, and only the highest values for each group are summarized in Fig. 1C. The inactivity level of the animals was scored on the basis of the method of Reuman et al. (70): 0, alert and playful; 0.5, alert but playful only when stimulated; 1, alert but not playful when stimulated; 2, neither alert nor playful when stimulated. A relative inactivity index of each cohort reported in Fig. 1C was calculated as follows: $\Sigma_{(\text{day 1 to day 14})}(\text{score} + 1)_n / \Sigma_{(\text{day 1 to day 14})} n$, where n equals the total number of observations from day 1 to 14 p.i. A value of 1 was added to each observation score, resulting in a value of 1.0 as the minimum number for the inactivity index. Healthy newly weaned and adult ferrets would receive the same minimum index of 1.0, as they are active and playful without the need for any incentive, despite the difference in their activeness.

Determination of viral load. Nasal washes were collected from the infected ferrets on days 3, 5, and day 7 p.i. and placed in nasal wash buffer (1% bovine serum albumin [BSA], 100 U/ml penicillin, and 100 μg/ml streptomycin in phosphate-buffered saline [PBS]). One milliliter of nasal wash buffer was used for each collection. Penicillin and streptomycin were obtained from Invitrogen Canada (Burlington, ON, Canada), and BSA was from Wisent Inc. (Saint-Bruno, QC, Canada). Tracheas and lungs were collected on days 3 and 7 p.i. from the euthanized ferrets. All the samples were stored at −80°C before processing. Viral replication in the upper, middle, and lower respiratory tract was assessed by endpoint titration of nasal washes or homogenized tissue samples from the infected ferrets in MDCK cells (50% tissue culture infective dose [$TCID_{50}$]) using hemagglutination as the readout for positive wells, as previously described (71). Briefly, nasal washes were diluted 1:10 in viral Dulbecco's modified Eagle's medium (vDMEM; containing 1% BSA, 25 mM glucose, 1 mM sodium pyruvate, 4 mM glutamine, 100 U/ml penicillin, 100 μg/ml streptomycin, 50 μg/ml gentamicin, and 1 μg/ml tosylsulfonyl phenylalanyl chloromethyl ketone [TPCK]-trypsin), followed by half-log serial dilution from $10^{-1.0}$ to $10^{-6.5}$ in quadruplicate with vDMEM on MDCK cells in 96-well flat-bottom plates (Sarstedt, Inc., Saint-Leonard, QC, Canada). Tissues were processed similarly, except that they were initially homogenized 1:10 (wt/vol) in suspension DMEM (sDMEM; vDMEM excluding 1% BSA) on ice and centrifuged before titration of the homogenates on MDCK cells. Before infection, MDCK cells were maintained in the log phase at low passage numbers and grew in cell DMEM (cDMEM; DMEM containing 10% fetal bovine serum, 25 mM glucose, 1 mM sodium pyru-

vate, 6 mM glutamine, 1 mM nonessential amino acids, 100 U/ml penicillin, and 100 μg/ml streptomycin). On the day before viral sample titration, 2×10^4 MDCK cells were seeded into each well to reach 95% confluence on the next day. After a 2-h incubation of titrated viral samples with MDCK cells at 37°C in 5% CO_2, samples were aspirated and replaced with fresh vDMEM, followed by a 6-day incubation at 37°C in 5% CO_2. On day 6 postincubation, supernatants were examined for the presence of virus by hemagglutination of 0.5% turkey erythrocytes (Lampire Biological Laboratories, Pipersville, PA). The viral titers were determined as the reciprocal of the dilution resulting in 50% hemagglutinin (HA) positivity in units of $TCID_{50}$s/ml represented in $\log_{10}$ base. All cell culture reagents were obtained from Invitrogen Canada, except for TPCK-trypsin (Sigma-Aldrich Canada Ltd., Oakville, ON, Canada).

Determination of influenza virus-specific antibody response. Sera were collected from infected ferrets on days 0, 3, 7, and 14 p.i. The influenza virus-specific antibody response from the uninfected or infected ferrets was measured by HI assay as previously described (35). Briefly, receptor-destroying enzyme (RDE; Accurate Chemical & Scientific Corp., Westbury, NY)-treated ferret antisera were half serially diluted, and the HI titer of each antiserum was determined to be the highest dilution that completely inhibited influenza virus hemagglutination of 0.5% turkey erythrocytes at 4 HA units. The presented value is the geometric mean of the HI titers from each group at each time point and represented by $\log_2$ base.

Complete leukocyte count. Blood was collected from live ferrets on days 0, 3, 7, and 14 after initial blood collection. Blood samples were collected in anticoagulant-containing tubes and analyzed in a Hemavet HV950FS multispecies hematology analyzer (Drew Scientific, Inc., Dallas, TX). The machine counted the number of each cell type, which was distinguished by the gated boundary of the cell volume and the inner complexity of the cell.

Histopathology and histoimmunochemistry. On day 7 p.i., animals were euthanized and the upper and lower left lobes of the lung tissues were harvested and formalin fixed by perfusion, followed by paraffin embedding and sectioning. Tissue slides were then stained with hematoxylin-eosin for histopathology assessment. Uninfected newly weaned and adult ferrets were also used for healthy and age-matched controls. Immunostaining was performed using a polyclonal rabbit anti-human CD3 (1:500; Dako Canada, Inc., Burlington, ON, Canada), followed by incubation with goat anti-rabbit IgG-horseradish peroxidase (HRP; 1:200; Jackson ImmunoResearch Laboratories, Inc., West Grove, PA) and polyclonal goat anti-dog IgA-fluorescein isothiocyanate (FITC; 1:1,000; AbD Serotec Ltd., Kidlington, United Kingdom), incubation with donkey anti-FITC IgG-HRP (1:1,000; Jackson ImmunoResearch Laboratories, Inc., West Grove, PA) and goat anti-ferret IgM (1:500; Rockland Immunochemicals, Inc., Gilbertsville, PA), and incubation with donkey anti-goat IgG-HRP (1:1,000; Jackson ImmunoResearch Laboratories, Inc., West Grove, PA). The scores for the iBALT-like structure were determined by randomly counting five different fields per section of one lobe under a magnification of ×40. The scores were averaged from the values for at least six lobes (two lobes per animals with at least three animals) per age group. The score represents the number of iBALT-like structures per field.

Preparation of lung protein lysates, Western blotting, and densitometry. Excised lung tissues were immediately frozen on dry ice and transferred to −80°C for storage before processing. Lung tissues were then homogenized in cell lysis buffer (50 mM Tris-HCl, pH 7.4, 150 mM NaCl, 1% Triton X-100, 0.25% sodium deoxycholate, 1 mM EDTA) containing complete protease inhibitor cocktail (Roche Diagnostics Ltd., Laval, QC, Canada). All the procedures were carried out on ice. Proteins were standardized using the Bradford assay (Bio-Rad Laboratories Canada Ltd., Mississauga, ON, Canada) and boiled in sampling buffer (62.5 mM Tris-HCl, pH 6.8, 10% glycerol, 2% SDS, 0.001% bromophenol blue, 1% β-mercaptoethanol) before loading onto the gel. After gel electrophoresis, the content was transferred to a nitrocellulose membrane using the semi-dry method, followed by appropriate blocking (5% nonfat dry milk in 0.05% Tween 20 in PBS [PBST]) before overnight incubation with the primary antibody in the blocking buffer at 4°C. After a sufficient wash with 0.05% PBST, the membrane was incubated with secondary antibody coupled to HRP in the same blocking buffer for 1 h at room temperature. After washing, the membrane was incubated with Pierce ECL Western blotting substrate (Thermo Fisher Scientific Inc., Rockford, IL) at room temperature for 1 min before exposure and film development in a darkroom. Rabbit anti-human myeloperoxidase (MPO; 1:2,000) was obtained from Upstate Cell Signaling Solutions (Millipore Canada Ltd., Etobicoke, ON, Canada). Mouse anti-human GAPDH (glyceraldehyde-3-phosphate dehydrogenase; 1:1,000), goat anti-rabbit IgG-HRP (1:10,000), and goat anti-mouse IgG-HRP (1:5,000) were obtained from Santa Cruz Biotechnology Inc. (Santa Cruz, CA). Films with bands that were not overexposed were used for densitometry using a GS-800 calibrated imaging densitometer system (Bio-Rad Laboratories Canada Ltd., Mississauga, ON, Canada) following the manufacturer's instruction. MPO values were normalized to GAPDH values, and the statistical analysis was performed on groups under the same exposure from the same blot.

RNA extraction and quantitative real-time PCR. RNA extraction and real-time PCR were performed as previously described (71). Briefly, lung tissues were excised and immediately kept in RNAlater solution (Ambion, Austin, TX), followed by storage at −80°C before processing. Lung tissues were then homogenized, and total RNA was isolated using an RNeasy minikit (Qiagen Canada Inc., Toronto, ON, Canada) according to the manufacturer's recommended protocol. Total RNA was converted into cDNA using an ImProm-II reverse transcription system (Promega Inc., Madison, WI), followed by quantitative real-time PCR. Real-time PCR of all the specified genes was performed in triplicate for each sample using an ABI Prism 7900HT system (Applied Biosystems, Foster City, CA). PCRs were performed using SYBR green PCR master mix (Applied Biosystems Inc., Carlsbad, CA) with cDNA and sets of primers specific for each gene, 40 amplification cycles, and an annealing temperature of 60°C. Gene expression levels were standardized according to the level for the corresponding housekeeping gene β-actin in the same sample and then normalized to the average for the standardized value for each gene for adults on day 0. The results were expressed as the fold change relative to the value for the adult on day 0.

Statistical analyses. An unpaired, two-tailed Student's *t* test was conducted for the data in Fig. 1 to 3, 5, 6, and 7B and C. A *P* value of ≤ 0.05 was considered statistically significant.

RESULTS

Newly weaned ferrets display mild clinical symptoms upon H1N1pdm infection. From clinical reports for pediatric H1N1pdm infection, disease severity in healthy children was determined to be moderate, and the majority of young children who suffered from severe H1N1pdm infections had accompanying physiological illnesses or abnormalities (2, 10, 37, 42, 61). In our study, healthy male influenza virus-naïve young (newly weaned, 5 to 8 weeks old) and adult (4 to 6 months old) ferrets were infected with influenza virus A/Mexico/4108/2009 (Mex/4108), an H1N1pdm strain that we have previously shown induces a severe clinical course in ferrets (35). Animals were infected at 10^6 EID_{50}s. Animals were monitored for clinical symptoms daily for 14 days p.i. The clinical parameters monitored included body temperature, weight, nasal discharge, sneezing, and inactivity level of the animals. The same parameters (excluding body temperature) were also monitored in an uninfected age-matched newly weaned cohort for 14 days as a baseline age-matched control. Uninfected animals did not experience weight loss (Fig. 1B), had a regular activity level, and had no incidence of nasal discharge and/or sneezing (data not shown).

Upon infection, adult ferrets developed an acute and intense

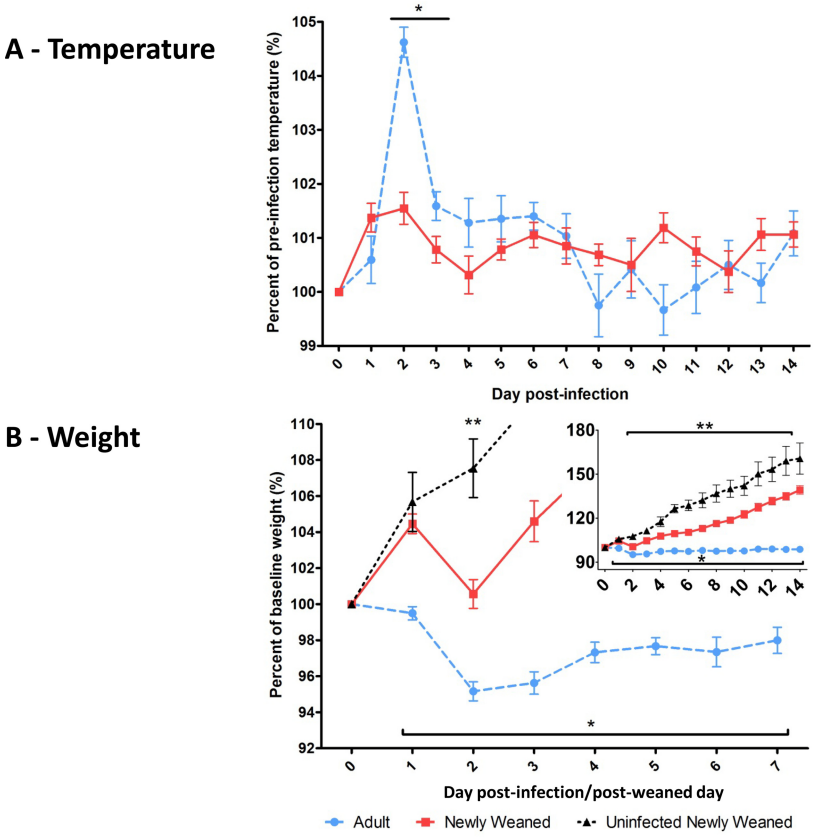

C

Clinical Sign	Adult	Newly Weaned
Nasal Discharge	75.0% (9/12)	60.9% (14/23)
Sneezing	33.3% (4/12)	25.0% (5/20)
Inactivity index	1.024	1.014

FIG 1 Reduced clinical illness in H1N1pdm-infected newly weaned ferrets. Clinical signs of A/Mexico/4108/2009 (10^6 EID_{50})-infected young ferrets ($n = 23$, 5 to 8 weeks old) and adult ferrets ($n = 18$, 4 to 6 months old) were measured daily over 14 days p.i. Temperature (A) and weight (B) were recorded daily until the last day and are expressed as a percentage relative to the average preinfection level calculated from the values on days 0 and −1. As a control, the body weights of uninfected newly weaned ferrets ($n = 13$, 5 to 8 weeks old) were monitored for 15 days and represented as a percentage relative to the average baseline level calculated from the values for the first 2 days of observation after they were weaned from their mothers. (B) The inset *x* axis is defined as days postinfection/post-weaning day and the *y* axis as percent baseline weight (%). (C) Animals were evaluated daily for nasal discharge, sneezing, and inactivity level, and the highest percentages (and fractions [number of ferrets displaying symptoms/total number of ferrets tested]) of infected ferrets displaying symptoms are shown. The physical inactivity index measures the degree to which ferrets respond to environmental stimuli, with the basal level being 1.000. Error bars represent standard errors of the means. *, $P < 0.05$ by Student's *t* test comparing infected adult to infected young ferrets; **, $P < 0.05$ by Student's *t* test comparing uninfected to infected young ferrets.

fever on day 2 p.i. which extended over the following 6 days (Fig. 1A). In contrast, newly weaned ferrets did not manifest a high fever on day 2 p.i. ($P < 0.05$) but had a slight increase in temperature on day 2 p.i. that then oscillated between 101% of the baseline temperature and the baseline temperature for the remainder of the observation period. Furthermore, there was a significant difference in weight between the two age groups from day 1 to day 14 p.i. Adult ferrets began to lose weight on day 1 p.i., and their weight did not return to the baseline level during the observation period of 14 days (Fig. 1B). Conversely, newly weaned ferrets experienced weight loss at day 2 p.i., although their weights never fell below the baseline and they quickly recovered, gaining weight over the baseline by day 3. Despite the significant weight difference between the young infected and young uninfected control group on day 2, the slopes of weight gain from both groups were parallel after day 3 p.i. (Fig. 1B), which suggested similar growth rates between the two groups. Other clinical features, such as the incidence of nasal discharge and sneezing and the inactivity level of infected animals, were higher in the adult cohorts (Fig. 1C). In summary, we found that newly weaned ferrets displayed milder clinical symptoms of H1N1pdm infection than the adult ferrets, which suggested that young ferrets display a milder clinical disease than adult ferrets.

Equivalent viral clearance and antibody responses between young and adult age groups. As described above, we found that young ferrets displayed a milder clinical disease when infected with H1N1pdm influenza virus. From these findings, we next wanted to investigate the viral burden of the upper and lower respiratory tracts and the antibody response of each age group following infection. Viral load was assessed in the nasal cavity,

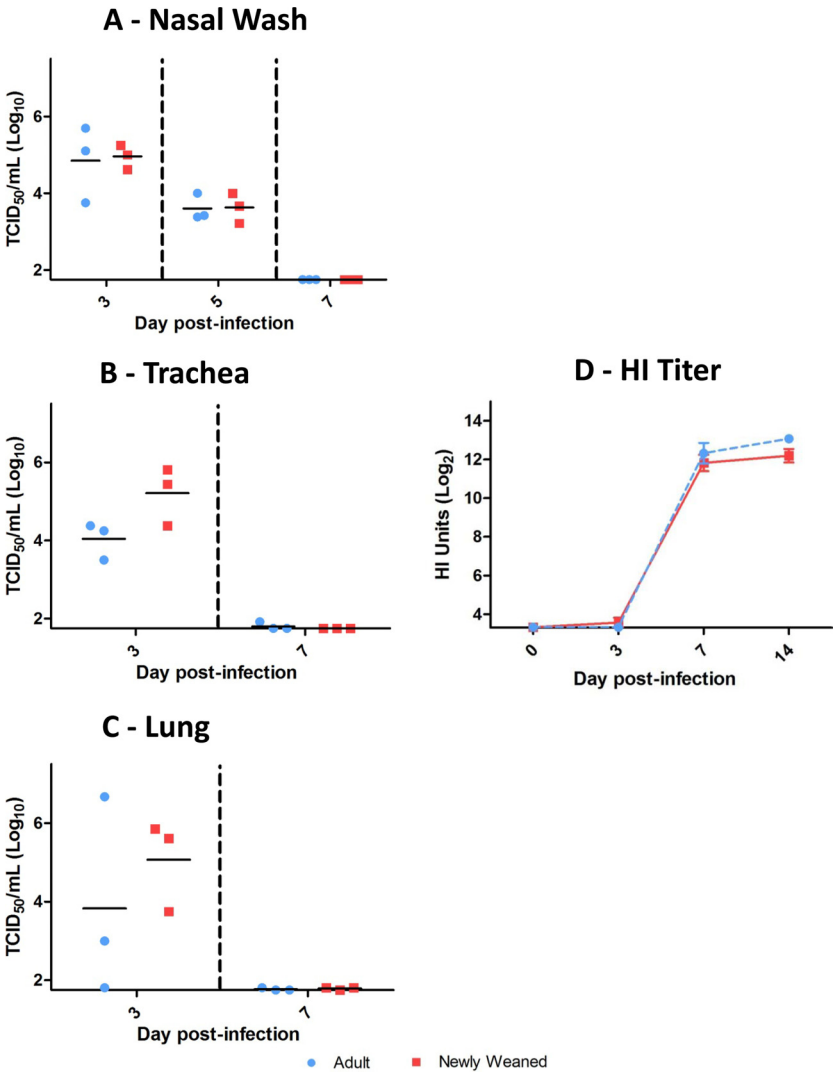

FIG 2 Equivalent viral clearance and influenza virus-specific antibody responses between adult and newly weaned ferrets. All nasal washes (A), tracheas (B), and lungs (C) from infected ferrets were collected on the specified days p.i. and processed before titrating on MDCK cells (number of $TCID_{50}$s/ml). A minimum of three samples from each time point were collected per group. Influenza virus-induced antibody kinetics in newly weaned and adult ferrets were measured by HI assay (D). Ferret antisera taken at the indicated days p.i. were used to measure the HI titer against live A/Mexico/4108/2009 virus. A minimum of three samples from each time point were collected per group. Error bars represent standard errors of the means.

trachea, and lung of infected animals. Interestingly, the viral titers from all locations were higher, although not significantly, in the newly weaned ferrets at the early time point (Fig. 2A to C). By day 7 p.i., both the newly weaned and adult ferrets were able to clear the virus throughout their respiratory tracts (Fig. 2A to C).

In addition to viral titers, we also wanted to determine if there was a difference in the B cell humoral response between the adult and newly weaned ferrets. Here we assessed the HA antibodies produced following infection in both age groups by HI assay. Upon Mex/4108 infection, anti-influenza virus HA antibody titers in both groups rose rapidly on day 7 p.i. and peaked by day 14 p.i. (Fig. 2D). We compared by enzyme-linked immunosorbent assay the influenza virus-specific IgG, IgA, and IgM levels in the lungs of the newly weaned versus adult ferrets using lung lysates. We found that in both groups, IgG and IgA levels peaked by day 14 p.i., but the differences between the two groups were not statistically significant (see Fig. S1 in the supplemental material). IgM levels in the newly weaned ferrets peaked on day 7 p.i. and were higher than those in adult ferrets. However, the comparison also showed no statistically significant differences. Therefore, the kinetics of influenza virus-specific immunoglobulins in the serum or lung were similar between the two groups. These results suggest that both the newly weaned and adult ferrets induced robust influenza virus-specific antibody responses, despite different clinical features.

Differential hematological leukocyte kinetics upon H1N1pdm infection between ferret age groups. Leukocyte cell population profiles in the peripheral blood are often suggestive of the health status of the animal and can give insight into the immune responses triggered during an infection. Here we investigated the white blood cell profile at baseline and during H1N1pdm infection. We sampled blood from the live infected newly weaned and adult ferrets on the specified days after H1N1pdm infection. Furthermore, we also measured the leuko-

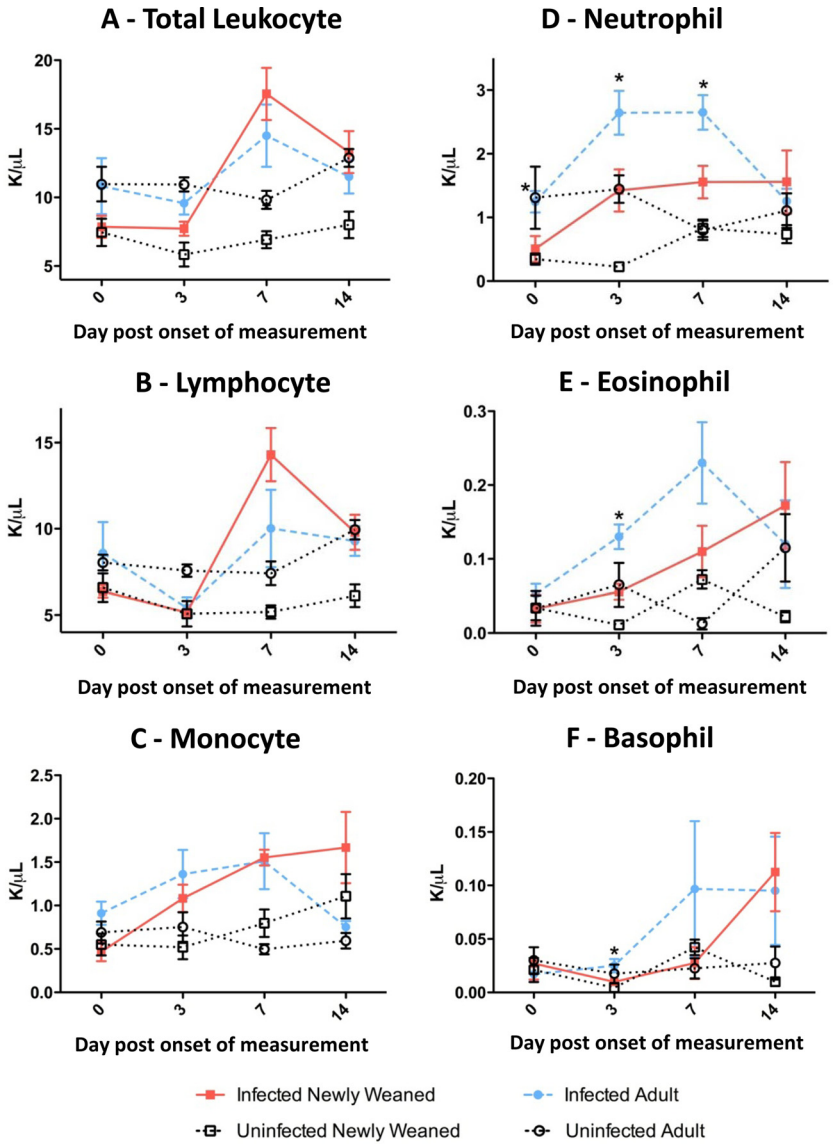

FIG 3 Two distinct types of hematological leukocyte kinetics among adult and newly weaned ferrets after H1N1pdm infection. Hematological cells were counted for total leukocytes (A), lymphocytes (B), monocytes (C), neutrophils (D), eosinophils (E), and basophils (F) in adult and newly weaned ferrets on the indicated days for 2 weeks after initial leukocyte sampling. A minimum of three samples from each time point were collected per group. K/μl, thousands of cells per microliter. Error bars represent standard errors of the means. *, $P < 0.05$ by Student's *t* test comparing infected adult and young ferrets on the same corresponding days.

cyte levels in blood from uninfected ferrets of the same ages as the infected ferrets to ensure that the change in the infected counterparts resulted from an infection.

Prior to infection, levels of total leukocyte and all cell populations except eosinophils and basophils were found to be higher in adults than newly weaned animals (Fig. 3). For the uninfected groups, minimum variation in the levels of all cell populations was observed after initial blood sampling within the 14-day observation period. However, upon H1N1pdm infection, the leukocyte kinetics bifurcated into two profiles between the two age cohorts (Fig. 3B to F). Lymphocyte and monocyte levels increased more rapidly (steeper slopes) postinfection in the newly weaned ferrets (Fig. 3B and C), where the lymphocytes reached their apex on day 7 p.i. and the monocytes reached their apex on day 14 p.i. Conversely, neutrophil, eosinophil, and basophil levels were significantly higher ($P < 0.05$) in the adults (Fig. 3D to F), peaking on day 3, day 7, and day 7, respectively. Importantly, the neutrophil level was substantially higher in the adults from days 0 to 7 p.i. (Fig. 3D). In summary, distinct leukocyte profiles in the peripheral blood were observed between the two age groups upon H1N1pdm infection, where high levels of inflammatory granulocytes were found in the infected adult ferrets.

Minimal lung pathology in infected newly weaned ferrets compared to significant inflammation in the lungs of infected adults. Following infection, we observed different blood cell profiles between the infected adult animals and the newly weaned ferrets. We have previously shown that infection with H1N1pdm in adult ferrets showed pronounced inflammatory cell infiltration

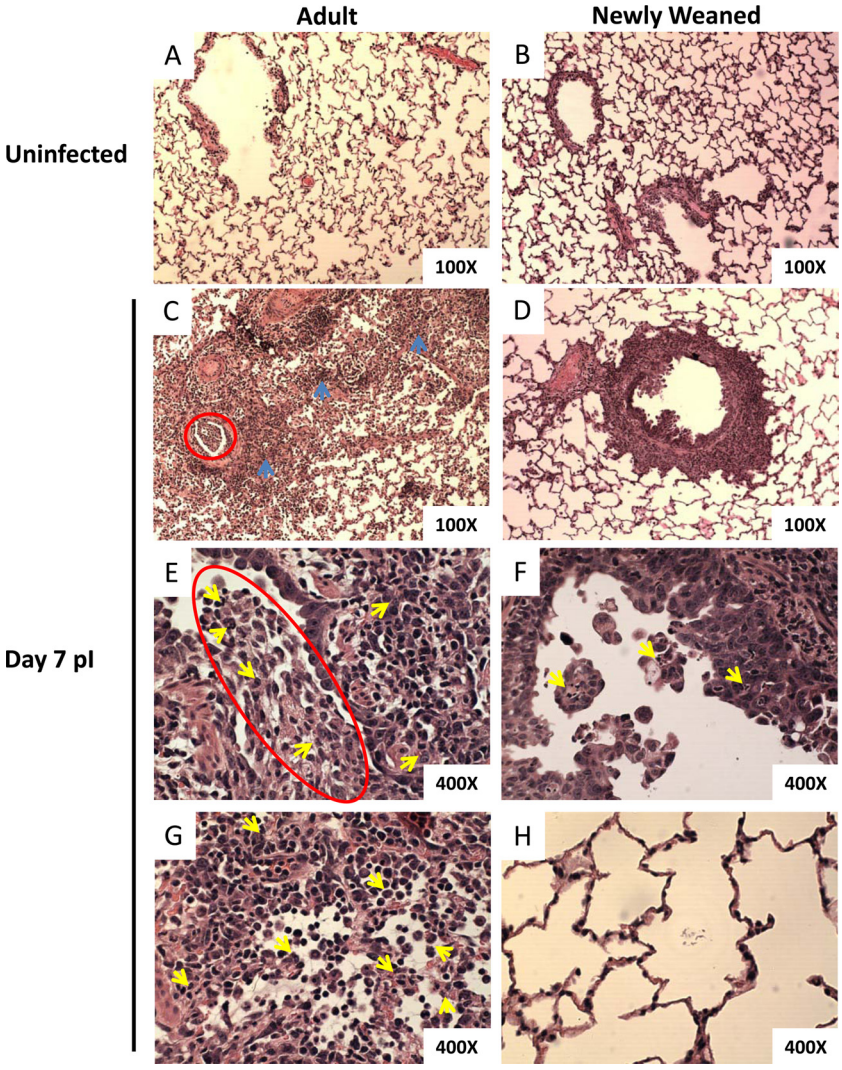

FIG 4 Early improvement of pulmonary histopathology in H1N1pdm-infected newly weaned ferrets. Hematoxylin-eosin (H&E) staining of paraffin-embedded lung sections from uninfected adult (A) and uninfected newly weaned (B) ferrets and from infected adult (C, E, and G), and infected newly weaned (D, F, and H) ferrets at day 7 p.i. Magnifications, ×100 (A to D) and ×400 (E to H). Representative images are shown for a minimum of three animals per group. Blue arrows, regions of intensive alveolar consolidation, hemorrhage, edema, and inflammatory exudates; red circles, bronchiolar exudates of inflammatory and epithelial cells and mucus; yellow arrows, infiltrated neutrophils.

and complementary pathological destruction in the lung by day 3, which continued to day 7 p.i. (35). We next went on to investigate the integrity of the lungs of both the adult and young animals following infection with H1N1pdm by histopathological analysis. By day 7 p.i., profound pneumonia was observed in numerous areas of the adult lungs, whereas in the lungs of newly weaned ferrets, the affected areas were mainly contained to the bronchiolar space (Fig. 4C to H). Furthermore, in the newly weaned animals, only minor desquamation of the cuboidal epithelial cells and debris plugs was observed in the bronchioles, unlike the pathology seen in the adult lung at day 7 (Fig. 4D and F). The majority of the young ferret alveoli appeared normal and similar to those in uninfected control ferrets (Fig. 4B, D, And H). Furthermore, by day 7 after H1N1pdm challenge, numerous discrete structures of mononuclear leukocyte aggregation not seen in the adult lung were found at the peribronchiolar and bronchiole-associated perivascular regions in the lungs of newly weaned ferrets (Fig. 4D; see Fig. 7A). In contrast, we observed intensive alveolar consolidation, hemorrhage, edema, and inflammatory exudates in several regions of the adult lungs (Fig. 4C, blue arrows). Sloughing of the epithelial cells, cellular debris of the inflammatory cells, fibrin, and a mucous plug were readily observed in the adult airway lumens (Fig. 4C and E, red circles). In addition, peribronchiolar, perivascular, and alveolar spaces were infiltrated with granulocytes and mononuclear cells in the adult lungs (Fig. 4C, E, And G). These leukocytes dissipated in the adult lungs in a disorganized manner and caused atelectasis of airway lumens. Most importantly, neutrophil infiltration was prominent in the bronchioles and alveoli and caused bronchiolitis and alveolitis (Fig. 4E and G, yellow arrows).

From these results, we next went on to measure the neutrophil-associated inflammatory response in the infected lungs. To investigate neutrophil infiltration in the lung, we quantified the neutrophil protein MPO levels in the lungs by Western blotting and

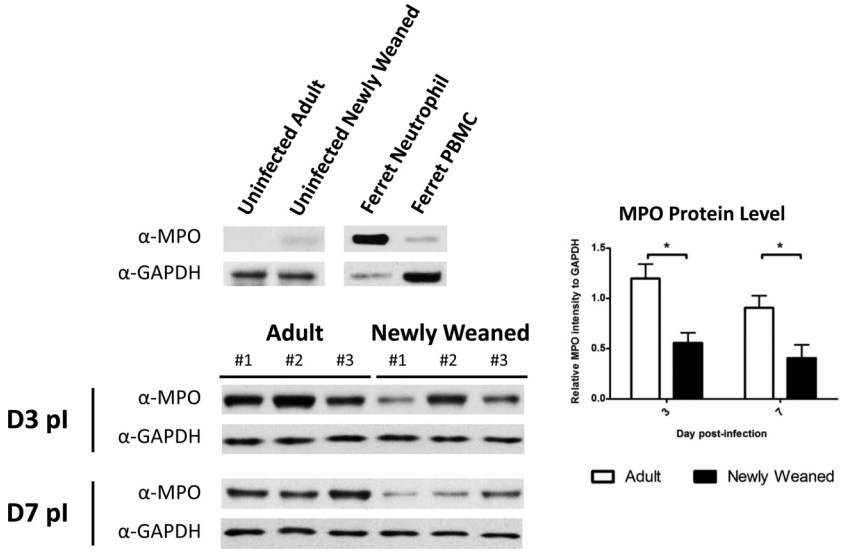

FIG 5 High levels of inflammatory MPO responses in adult ferrets infected by H1N1pdm. Western blot analysis was performed for the detection of MPO and GAPDH proteins in the lungs of newly weaned and adult ferrets. The densitometry readout of the MPO band was normalized to that of the corresponding GAPDH band of the same animal. The average of normalized readouts is shown for each group on days 3 and 7 p.i. A minimum of three lung samples were collected at each time point per group. *, $P < 0.05$ by Student's *t* test comparing groups on the same day p.i. PBMC, peripheral blood mononuclear cells.

densitometry. MPO is mainly expressed in neutrophils and plays an important role in oxidative burst reactions by neutrophils (41, 59, 81). Control blots showed antibody specificity to positive-control ferret neutrophils and no reactivity toward ferret lymphocyte cell lysate (Fig. 5, top). Analysis of lung homogenates of 3 ferrets from each group showed that MPO levels were significantly lower in the lungs of newly weaned ferrets on day 3 and day 7 p.i. (Fig. 5) than in adult lung tissue. These results were quantified by densitometry, which showed that adults had a significantly larger amount of MPO in lungs on day 3 and day 7 than the young ferrets.

Differential inflammatory and regulatory immune responses in the H1N1pdm-infected lungs of both cohorts contribute to the pathological differences. Inflammatory responses upon viral infection, such as the expression of interferon-stimulating genes (ISGs), enhance antiviral immunity and the recruitment and activation of leukocytes to the site of infection for viral clearance (17, 23, 34). Signature ISGs include 2′-5′-oligoadenylate synthetase-like (OASL), CXCL9, CXCL10, and major histocompatibility complex (MHC) genes. The responses of regulatory cytokines, such as IL-10 and TGF-β, dampen and modulate the inflammatory responses to balance the destructive nature of inflammation in the host. Since our analysis showed differences in the histopathology and blood cell profiles, we went on to examine the expression of genes involved in the inflammatory and regulatory responses in the lung upon infection between both newly weaned and adult ferrets.

RNA was extracted from newly weaned and adult ferret lungs on days 0, 3, 7, and 14 after H1N1pdm infection and was subjected to real-time PCR for ISG and IL-10 and TGF-β1 gene expression. We found that these genes were highly expressed on day 3 p.i. in newly weaned ferrets (OASL, CXCL9, IL-10, and TGF-β1 gene expression in newly weaned ferrets was significantly higher than that in adult ferrets) and that their expression gradually decreased along the time course (Fig. 6Ai, Aii, and B). The result of differential ISG responses between the two groups prompted us to examine MHC expression in the lung upon infection, as influenza virus infection is known to inhibit MHC presentation (21). Furthermore, upon infection, young and adult animals have been shown to have a distinct, preferred T cell epitope hierarchy in relation to MHC (72). Here we wanted to know if H1N1pdm infection may also alter the MHC expression profile between the two age groups. Interestingly, MHC expression in the adults had a delayed elevation on day 7 p.i. and onward, and the level was significantly higher than the level of MHC expression in the newly weaned ferrets, where their MHC expression level peaked at day 3 p.i. (Fig. 6Aii). In summary, these results showed that the ISG and regulatory gene profiles in newly weaned ferrets differed significantly from those in the adult ferrets upon H1N1pdm infection.

Formation of immune cell organizations in the lungs of H1N1pdm-infected newly weaned ferrets. Leukocyte infiltration into the lung is one of the signature inflammatory responses upon influenza virus infection (24, 27, 35, 36, 55, 58, 77). Although leukocyte infiltration can remove pathogens from the infected site, this process can also lead to intensive tissue damage if the response is not controlled. iBALTs, like other ectopic lymphoid organs in species such as humans and mice, are formed following infection or persistent stimulation by leukocyte recruitment to the lung (19, 31, 56, 91). The structure, unlike random cell infiltration, is organized and usually localized at the site of infection.

In our ferret model, BALT-like structures were not readily observed in either the healthy uninfected adult or uninfected newly weaned group (Fig. 4A and B). However, by day 7 after H1N1pdm challenge, numerous discrete structures of mononuclear leukocyte aggregation were found at the peribronchiolar and sometimes bronchiole-associated perivascular regions in the lungs of newly weaned ferrets (Fig. 4D and 7A). Similar structures were also observed at the lamina propria surrounding some regions of bronchi (data not shown). Conversely, these structures were not prominently identified in adult lungs.

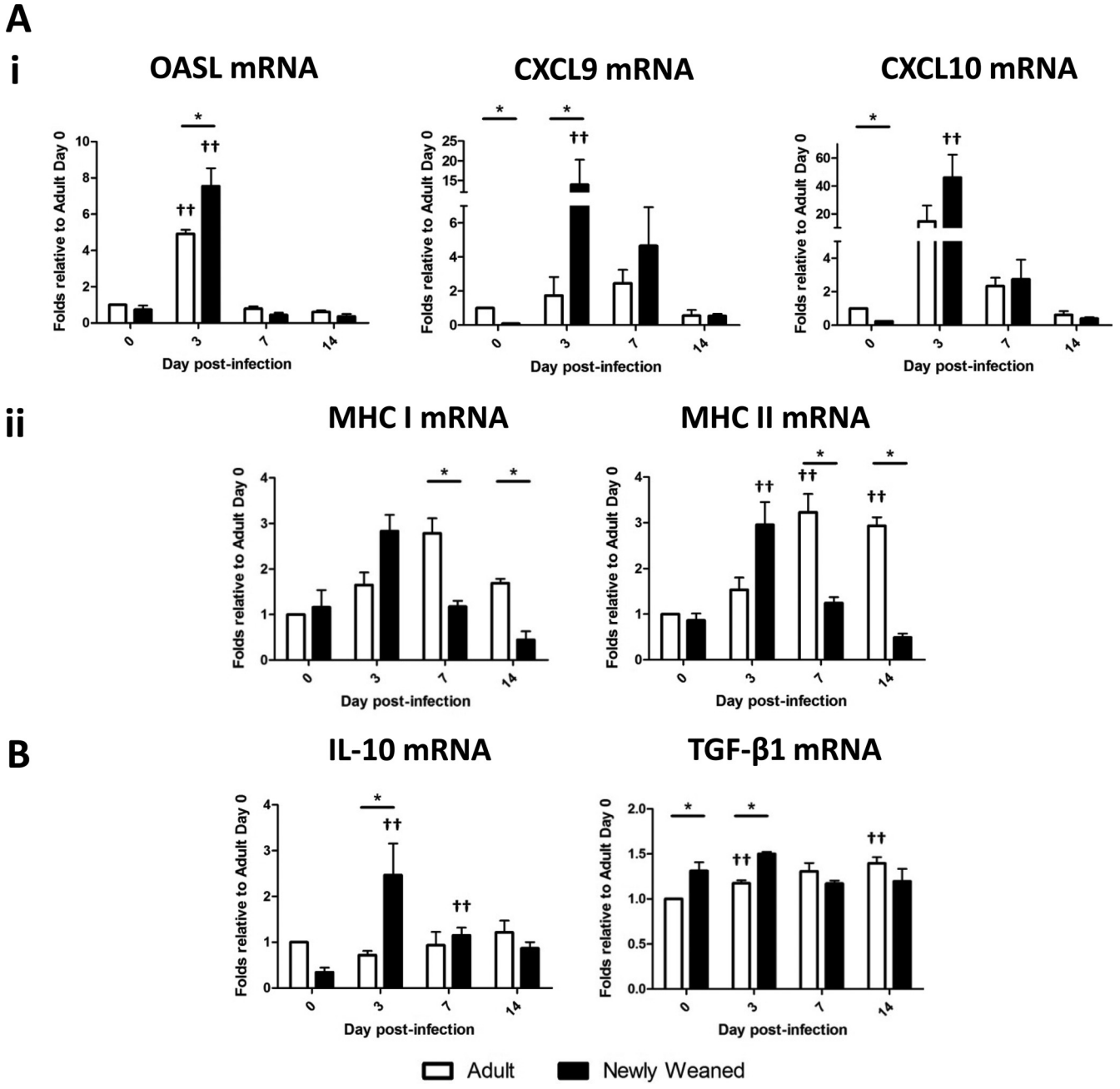

FIG 6 Differential ISG and regulatory cytokine responses between ferrets in the two age groups upon H1N1pdm infection. Expression of ISGs OASL, CXCL9, and CXCL10 (i) and MHC class I and MHC class II genes (ii) (A) and genes for regulatory cytokines (IL-10 and TGF-β1) (B) was measured by real-time PCR. Triplicate analyses were performed for all genes in each sample, and the results were averaged. The resultant averaged values were first standardized to each corresponding β-actin gene level and then normalized to the average of the standardized value for each gene for adults on day 0. A minimum of three lung samples were collected at each time point per group. Error bars represent standard errors of the means. *, $P < 0.05$ by Student's *t* test comparing groups on the same day p.i.; ††, $P < 0.05$ by Student's *t* test comparing day 0 and the indicated day p.i. of the same age group.

We scored the number of iBALT-like structures for each age group to demonstrate their prevalence in the lungs of H1N1pdm-infected newly weaned ferrets. In general, we found in the range of 3 to 5 iBALT-like structures per field in the newly weaned ferret lungs. In contrast, iBALT-like structures were absent in most fields in the adult lungs. The difference reached statistical significance ($P < 0.000001$) (Fig. 7B). To further investigate the makeup of these structures, we stained the infected and uninfected lungs from both age groups to identify the immune cell types that are associated with the iBALT architecture. At present, there is a paucity of ferret immune-specific reagents that are required for immunological profiling in the ferret. We performed immunohistochemistry on the lungs of infected and uninfected adult and young ferrets using antibodies for CD3, IgM, and IgA (Fig. 7A). The bronchi and bronchioles in the lungs of both the young and adult uninfected controls stained negative with these antibodies (data

not shown). At day 7 p.i., newly weaned ferret lung tissue showed positive CD3 staining in the cells surrounding the bronchioles, signifying T cells. Moreover, the cell clusters adjacent to the CD3-positive areas stained positive with the IgA and IgM antibodies, identifying B cells (Fig. 7A, red arrows). In contrast to the young ferret lung sections, in the infected adult counterpart, $CD3^+$ cells and IgA-positive (IgA^+)/IgM-positive (IgM^+) cells disseminated into the peribronchiolar and alveolar spaces. As well, the $CD3^+$ and IgA^+/IgM^+ cells of the adult lung were not found in an unorganized architecture in adjacent areas.

From these histological data, we wanted to know if the organized or confined structures of these lymphocyte aggregations in newly weaned ferret lungs were due to a unique chemokine response or simply a lower degree of T and B lymphocyte recruitment to the lungs in the newly weaned ferrets than in the adults. We quantified transcripts known to be expressed by T and B cells, such as CD3e and CD19, and the chemokines, such as CCL19, CCL21, and CXCL13, that are known to be involved in T and C cell structure formations, for instance, iBALT organogenesis. CD11c represents conventional dendritic cells. From the real-time PCR analysis, no statistically significant differences were seen for CD3e, CD19, and CD11c (Fig. 7C). Although the difference in CCL21 expression levels was also not significant, we found that CCL19 and CXCL13 were significantly upregulated in the lungs of newly weaned ferrets on day 3 p.i. (Fig. 7C). Taken together, these results suggested the possible regulation of T cells and B cells in H1N1pdm-infected newly weaned ferret lungs through a unique chemokine network.

DISCUSSION

Our study is the first to demonstrate milder H1N1pdm clinical disease in young animals than their adult counterparts. Importantly, these clinical observations in our ferret animal model paralleled the clinical observations for humans from the 2009 H1N1 influenza virus pandemic which reported that children had milder clinical symptoms than adults (32, 45, 52, 78, 89, 98, 99). Further investigation of this age-related differential disease pathogenesis in our ferret model revealed that although both newly weaned and adult ferrets cleared the viral infection at a similar rate, the blood cell profiles differed markedly between the groups and the resulting lung pathology was more severe in the adults. Moreover, histopathological analysis suggested the organization of immune cells in the lungs of the young animals resembling an iBALT-like structure, which was not seen in the adults. Taken together, these findings suggested that the unique clinical outcome of H1N1pdm infection in children may be indicative of the differential immunological mechanisms in their developing immune systems compared to those in the immune systems of adults. It is possible that their unique pathological and immunological responses can be extrapolated to be the protective signature against H1N1pdm infection. Importantly, the pediatric approach to influenza virus infection remains complex, and further work is needed to dissect the critical players in the pathogenesis. We have provided novel findings on the clinical and mechanistic responses in newly weaned ferrets following severe H1N1pdm influenza virus infection. Furthermore, these findings relate directly to the human population, highlighting the need for further investigation of the immature and developing immune system.

Asphyxia can affect children infected with influenza virus (1, 9, 16). Asphyxia is described as pneumonia that destroys the lung

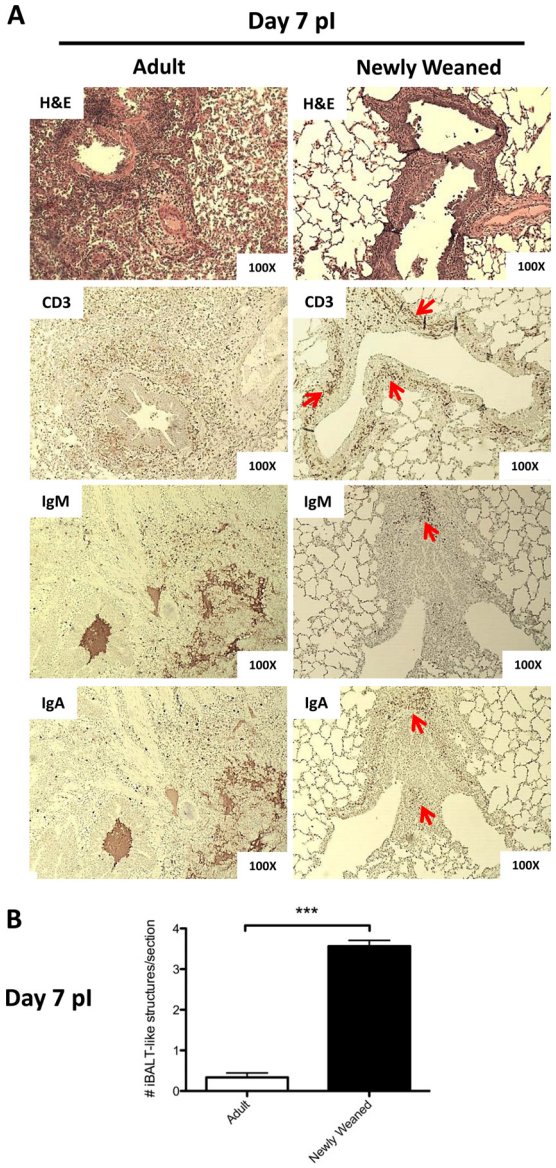

FIG 7 Induction of iBALT-like structures in the lungs of H1N1pdm-infected newly weaned ferrets. (A) Paraffin-embedded lung sections from infected adult and newly weaned ferrets from day 7 p.i. were analyzed by hematoxylin-eosin (H&E) staining and immunohistochemistry. Representatives are shown for all stainings at a magnification of ×100 for a minimum of three animals per group. Red arrows, cell cluster regions that stained positive for specific antigens. Anti-CD3 was used to identify T cells, and both anti-IgA and anti-IgM were used to identify B cells. (B) The numbers of iBALT-like structures per field represent the average score of the structure from five random fields per section of one lobe under a magnification of ×40. The average scoring included at least six lobes (two lobes per animals with at least three animals) for each age group. (C) Expression of genes for lymphocyte markers and homeostatic chemokines was measured by real-time PCR. Triplicate analyses were performed for all genes of each sample, and the results were averaged. The resultant averaged values were first standardized to each corresponding β-actin level and then normalized to the average of the standardized value for each gene for adults on day 0. A minimum of three lung samples were collected at each time point per group. Error bars represent standard errors of the means. *, $P < 0.05$ by Student's *t* test comparing groups on the same day p.i.; ***, $P < 0.000001$ by Student's *t* test comparing groups on the same day p.i.; ††, $P < 0.05$ by Student's *t* test comparing day 0 and the indicated day p.i. of the same age group.

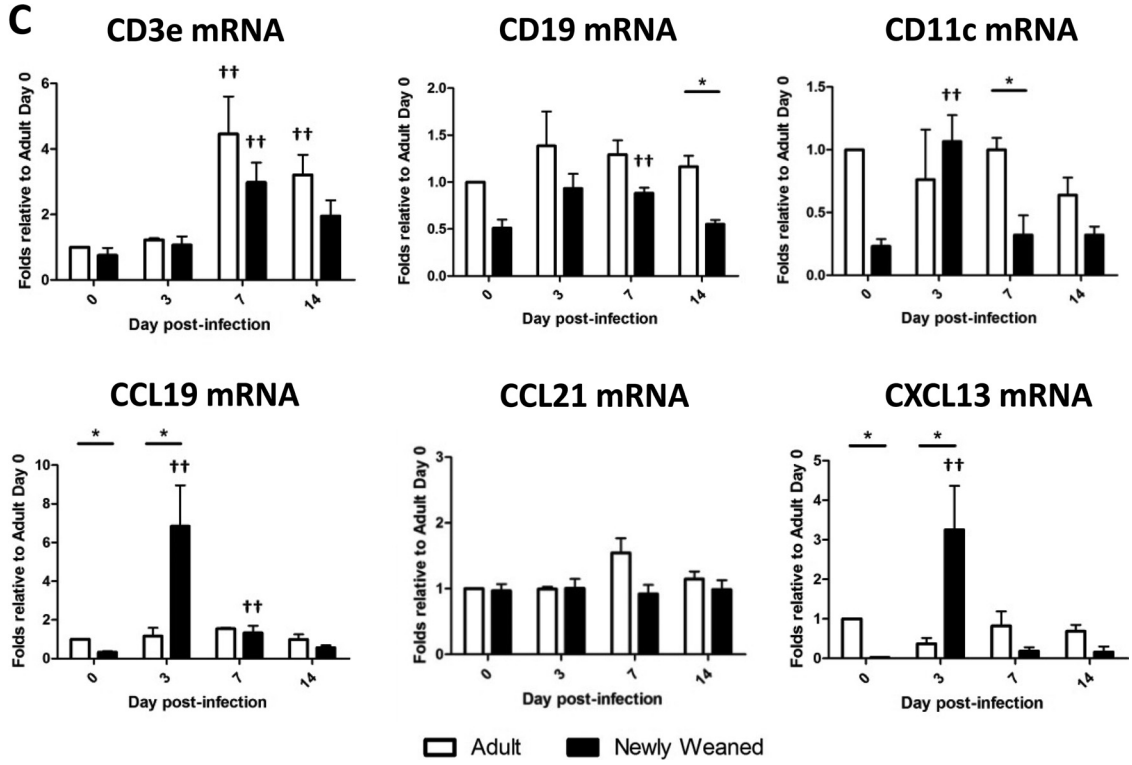

FIG 7 continued

architecture and occludes the airways, and this occlusion prevents efficient gas transfer. In the very young, the lung structure is composed of a smaller ratio of alveolar cells to ciliated epithelial cells compared to that in the lungs of adults. Furthermore, the airway spaces of children are, in general, smaller than those of adults (1, 16). Therefore, influenza virus-induced pneumonia in the young lung commonly causes airway obstruction and leads to a greater risk of asphyxia in newborns and infants. Moreover, children suffering from chronic respiratory conditions such as asthma also have restricted airways and are at a higher risk for complications associated with influenza virus infections. In our newly weaned ferret model, however, the young ferrets displayed a significantly milder disease following influenza virus infection. Even though the airway spaces were slightly smaller in the newly weaned ferrets, the majority of the alveolar structure remained intact upon H1N1pdm virus infection and bronchiolar space obstruction was not prominent. Although we did not measure respiratory rates, we did not observe any direct shortness of breath among the newly weaned ferrets. Respiratory failure due to a pulmonary structural defect or underdevelopment did not occur in our newly weaned ferret model.

From our viral titers and clinical observations, it appeared that newly weaned ferrets were significantly infected with the H1N1pdm virus and were able to clear the infection at a rate similar to that for the adult ferrets. Nevertheless, their lung pathology was less traumatic. One postulation was that the milder clinical symptoms and pneumonia resulted from the activation/inactivation of the young ferrets' underdeveloped immune system (11, 15, 44, 69, 94, 95). From our hematology data on the composition of peripheral blood cells, the levels of lymphocytes, monocytes, and neutrophils before infection were lower in the newly weaned ferrets than in the adults. Although this profile may suggest a premature immune system in the newly weaned ferrets, upon H1N1pdm infection, levels of lymphocyte and monocytes were acutely raised in these young ferrets. In addition, newly weaned ferrets elicited more active ISG responses in the lungs, and the level of the H1N1pdm-specific antibody response rivaled that in adult ferrets. Furthermore, while both groups were infected with the same infectious dosage, the newly weaned ferrets, which were smaller than the adult ferrets, were capable of clearing virus at a rate similar to that for the adults, again suggesting that the newly weaned ferrets had a robust immune system to eliminate infection. These results demonstrate that there was no deficiency in the immune system of the young ferrets and that they were able to elicit a strong antiviral response to clear the influenza virus infection.

When active immune responses are uncontrolled, they become pathogenic. Our pathological findings for H1N1pdm infection in the adult ferrets were in agreement with previous observations of the severe outcomes of H1N1pdm infection in humans, mice, and ferrets (24, 27, 35, 36, 55, 58, 71, 77). Here we observed severe pneumonia (interstitial pneumonia and bronchiolitis) with alveolar consolidation, hemorrhage, edema, and inflammatory debris in the airway spaces in adult lungs. Granulocyte infiltration was also prominent in the airways of the adult lungs. While neutrophils have been suggested to play an important role in viral clearance and be beneficial to the host (29, 30, 85–87, 92), several studies have also demonstrated that persistently high levels of neutrophils are pathogenic in influenza virus infections. In the studies using canine and mouse species, high neutrophil levels in

the lungs after influenza virus infection have been associated with severe lung pathology and a fatal outcome of the infection (39, 51, 59, 64, 76). Furthermore, Okada et al. (60) demonstrated high neutrophil levels in the blood that correlated with severe cases of H1N1pdm infection in pediatric patients. Tate et al. (87) used a monoclonal antibody, 1A8 (anti-Ly6G), to specifically deplete neutrophils in mice and rescued the animals from virulent PR8 influenza virus infection. In our study, in addition to the prominent neutrophil infiltration in the lung, severe inflammatory responses in the adults were evidenced by the persistence of high pulmonary MPO levels postinfection. MPO depletion in mice has also been shown to improve influenza virus pathogenesis (81); therefore, persistently high MPO levels in the adult ferrets suggested the pathogenic effect of this neutrophil enzyme during H1N1pdm infection. An overwhelming respiratory burst by MPO can exhaust the host and exacerbate tissue damage. Unfortunately, there is no commercialized antibody currently available for ferret neutrophils or MPO depletion to test this hypothesis in ferrets. While MPO levels were consistently high in the adult ferrets, MHC expression kinetics differed between the two groups. It is known that influenza virus infection alters MHC presentation in dendritic cells and that animals of different age groups have distinct repertoires of T cell receptor-peptide-MHC recognition (21, 72). It is not clear if the MHC expression level may also be altered between the two age groups upon H1N1pdm infection. From our results, we found that the kinetics of MHC expression in newly weaned ferrets were in parallel to the viral burden kinetics, which suggested the induction of viral clearance in the infected host cells in newly weaned ferrets. Conversely, the increase in the level of MHC expression in adult ferrets was after viral clearance. It is possible that this phenomenon resulted from delayed phagocyte infiltration. Alternatively, it can also be speculated that MHC-positive cells were involved in the clearance of cells damaged because of the intensive inflammatory responses in the adults (21, 25, 54). The kinetics of the hematological profile in the adults (high neutrophil and eosinophil levels) also demonstrated excessive inflammatory characteristics upon H1N1pdm infection. Several studies (39, 51, 59, 60, 76, 87, 88) have shown that elevated neutrophil and eosinophil levels contribute to the exacerbation of influenza virus pathogenesis. Furthermore, from the association of eosinophils and basophils to the H1N1pdm comorbidity factor, such as asthma in humans (2, 6, 10, 42, 60), higher levels of these granulocytes in the peripheral blood may play a role in severe H1N1pdm pathogenesis in adults. It is likely that high levels of neutrophils in the peripheral blood of adult ferrets contributed to the high MPO levels in their lungs. Taken together, these results show different pathological and hematological profiles between the adult and newly weaned H1N1pdm-infected ferrets.

Our results showed significantly reduced cellular and molecular responses in our newly weaned ferret model, and together with the restricted pathology, it is possible that an unknown additional regulatory mechanism contained the excessive inflammatory responses in the young ferrets. It has previously been demonstrated in several mouse studies that the neonatal immune system is highly regulated and these regulatory responses are more readily responsive than immune regulation in adults (82, 97, 100, 101). Regulatory lymphocytes or stromal cells dampen the destructive inflammatory actions caused by macrophages and dendritic cells through secretion of IL-10 or TGF-β. In addition, it has recently been shown that neonatal human serum contains factors that polarize IL-10 responses (5). Our data are in agreement with the current observations that IL-10 and TGF-β1 levels are significantly higher in young ferrets upon H1N1pdm infection. Moreover, it has also been suggested that robust interferon responses can reduce neutrophil influx into the lungs (76). This finding was in parallel to the lower MPO response that we saw in the lungs of newly weaned ferrets, where we found higher interferon responses. It is possible that the robust interferon responses dampen the pathogenic effect of neutrophil infiltration and contribute to the mild clinical outcome in the newly weaned ferrets. Furthermore, interferon responses have also been shown to enhance neonatal regulatory B cell functions to protect against lethal inflammation (100). Taken together, we found that the reduced inflammatory responses in the newly weaned ferrets resulted from a possible regulatory immunomodulation network in newly weaned ferrets to control H1N1pdm infections.

iBALT is defined by the location of the structure, organized cell types, and chemokine network that are involved. Here we found the formation of organized structures strictly surrounding the bronchi and bronchioles of the infected lungs of young ferrets, and we propose that these are a robust iBALT-like formation. iBALT is considered an inducible ectopic lymphoid organ that encompasses B and T cell zones which are adjacent to each other for the purpose of priming the adaptive immune responses (18, 19, 28, 66, 67, 74). In our newly weaned ferret model, the induction of this structure was triggered by H1N1pdm infection, and we hypothesize that an iBALT-like structure was formed to initiate anti-H1N1pdm adaptive responses. Interestingly, T and B cells were also recruited to the lungs of infected adults, but there was no defined organization or structure of these lymphocyte aggregations. Instead, these cells were disseminated and sometimes obstructed the airways. From our results, we show that the difference in the organization of lymphocyte recruitment between the two age groups is not due to different lymphocyte levels but perhaps results from the CCL19 and CXCL13 chemokine network. Importantly, Moyron-Quiroz and colleagues (56) have demonstrated that induction of iBALT alone was sufficient to protect mice from lethal influenza virus infection even in the absence of secondary lymphoid organs. Furthermore, the CCL19/21 and CXCL13 chemokine network in the lung not only is important for iBALT formation but also has been shown to have a protective role against severe disease in the host (68). In opposition to our work, a study by Sun et al. (83) demonstrated that young mice were more susceptible to H1N1pdm infection and developed more severe lung pathology. These authors found that iBALT was formed more readily in the adult mice than in newly weaned mice. The differences of pathogenesis and secondary structure formation in the lung may be explained by an immune response specific to the ferret or an age-specific window of requirements that were not matched to our study. Nevertheless, one common observation was that the animals that triggered sufficient iBALT-like structures developed a milder illness following H1N1pdm infection. It is possible that the iBALT configuration could differ by species, age, disease state, and inflammatory/infection stimulus, thereby altering the resultant iBALT appearance and structure (18, 19, 22, 26, 66, 67, 74), although an important commonality in all reported iBALT structures is their organized architecture, which seems to be central to their protective function. Furthermore, Moyron-Quiroz et al. (56) have demonstrated that when iBALT formation was not organized following influenza virus infection,

the clinical outcome deteriorated. Importantly, in our work, iBALT-like formation was specific to the newly weaned ferrets, which were associated with infection with a milder pathology. It is possible that in our model the iBALT-like structures were responsible for the regulation and organization of the effector anti-H1N1pdm adaptive immune responses in the defined areas to efficiently clear the infection with minimal tissue damage. Moreover, the absence of the iBALT-like networks in the adults may have contributed to the increased pathogenesis of H1N1pdm infection. More work is needed to investigate the role of iBALT in studies of H1N1pdm infection in the ferret and other animal models by age.

Newly weaned ferrets in our model of H1N1pdm infection demonstrated a milder clinical disease following infection with H1N1pdm which was similar to the disease described in human infants and children infected with 2009 H1N1 pandemic viruses. Here we investigated the possible mechanisms that dampened the severe outcome of H1N1pdm infection and found an increased neutrophil response in adults and the formation of iBALT-like structures accompanied by a unique regulatory and chemokine network in the lungs of the newly weaned ferrets. Future work could be performed to investigate the contribution of these ferret molecules in the context of H1N1pdm pathogenesis. Antibodies that can recognize ferret cytokines and chemokines need to be further characterized to determine if these antibodies can neutralize or deplete ferret molecules *in vivo* to test the hypothesis. Ferrets are a superlative model for studying respiratory diseases. When infected with respiratory viruses, ferrets display many of the symptoms and pathological features seen in infected humans, as ferrets and humans have similar lung physiology (4, 12, 40, 48, 53, 63). In regard to reagent development, it will take time for ferret reagent repositories to become as extensive as they are now for the mouse. We also investigated the expression profiles of genes for several other important immune mediators, such as several signature proinflammatory cytokine markers (tumor necrosis factor alpha, IL-1β, CCL2, CCL4, and CCL5); T_h1, T_h2, and T_h17; and antibody responses. In this analysis, we did not observe significant differences in these responses between the two age groups postinfection (data not shown). The discovery of a mild disease model in newly weaned ferrets offers new insights into the immature and developing immune system and has direct implications for adult and childhood respiratory illnesses, including the production of effective prophylactic treatments.

ACKNOWLEDGMENTS

We thank the Li Ka-Shing Foundation of Canada, Immune Diagnostics & Research, and Shantou University Medical College for support for conducting this study.

A/Mexico/4108/2009 virus was obtained through the Influenza Reagent Resource, Influenza Division, WHO Collaborating Center for Surveillance, Epidemiology and Control of Influenza, Centers for Disease Control and Prevention, Atlanta, GA.

We declare no conflict of interest.

REFERENCES

1. **Agrons GA, Courtney SE, Stocker JT, Markowitz RI.** 2005. From the archives of the AFIP: lung disease in premature neonates: radiologic-pathologic correlation. Radiographics **25**:1047–1073.
2. **Bagdure D, Curtis DJ, Dobyns E, Glode MP, Dominguez SR.** 2010. Hospitalized children with 2009 pandemic influenza A (H1N1): comparison to seasonal influenza and risk factors for admission to the ICU. PLoS One **5**:e15173. doi:10.1371/journal.pone.0015173.
3. **Baker MG, et al.** 2009. Pandemic influenza A(H1N1)v in New Zealand: the experience from April to August 2009. Euro. Surveill. **14**(34): pii=19319. http://www.eurosurveillance.org/ViewArticle.aspx?ArticleId=19319.
4. **Banner D, Kelvin AA.** 2012. The current state of H5N1 vaccines and the use of the ferret model for influenza therapeutic and prophylactic development. J. Infect. Dev. Ctries. **6**:465–469.
5. **Belderbos ME, et al.** 2012. Neonatal plasma polarizes TLR4-mediated cytokine responses towards low IL-12p70 and high IL-10 production via distinct factors. PLoS One **7**:e33419. doi:10.1371/journal.pone.0033419.
6. **Brusselle GG, Joos GF, Bracke KR.** 2011. New insights into the immunology of chronic obstructive pulmonary disease. Lancet **378**:1015–1026.
7. **Coates DM, Husseini RH, Collie MH, Sweet C, Smith H.** 1984. The role of cellular susceptibility in the declining severity of respiratory influenza of ferrets with age. Br. J. Exp. Pathol. **65**:29–39.
8. **Coates DM, Husseini RH, Rushton DI, Sweet C, Smith H.** 1984. The role of lung development in the age-related susceptibility of ferrets to influenza virus. Br. J. Exp. Pathol. **65**:543–547.
9. **Collie MH, Rushton DI, Sweet C, Smith H.** 1980. Studies of influenza virus infection in newborn ferrets. J. Med. Microbiol. **13**:561–571.
10. **Cox CM, Blanton L, Dhara R, Brammer L, Finelli L.** 2011. 2009 pandemic influenza A (H1N1) deaths among children—United States, 2009-2010. Clin. Infect. Dis. **52**(Suppl 1):S69–S74.
11. **Cupedo T.** 2011. Human lymph node development: an inflammatory interaction. Immunol. Lett. **138**:4–6.
12. **Darnell ME, et al.** 2007. Severe acute respiratory syndrome coronavirus infection in vaccinated ferrets. J. Infect. Dis. **196**:1329–1338.
13. **Dawood FS, et al.** 2009. Emergence of a novel swine-origin influenza A (H1N1) virus in humans. N. Engl. J. Med. **360**:2605–2615.
14. **Ding Q, et al.** 2011. Regulatory B cells are identified by expression of TIM-1 and can be induced through TIM-1 ligation to promote tolerance in mice. J. Clin. Invest. **121**:3645–3656.
15. **Drayton DL, Liao S, Mounzer RH, Ruddle NH.** 2006. Lymphoid organ development: from ontogeny to neogenesis. Nat. Immunol. **7**:344–353.
16. **Dunnill M.** 1962. Postnatal growth of the lung. Thorax **17**:329–333.
17. **Ehrhardt C, et al.** 2010. Interplay between influenza A virus and the innate immune signaling. Microbes Infect. **12**:81–87.
18. **Fleige H, et al.** 2012. Induction of BALT in the absence of IL-17. Nat. Immunol. **13**:1. doi:10.1038/ni.2167.
19. **Foo SY, Phipps S.** 2010. Regulation of inducible BALT formation and contribution to immunity and pathology. Mucosal Immunol. **3**:537–544.
20. **Fraaij PL, Heikkinen T.** 2011. Seasonal influenza: the burden of disease in children. Vaccine **29**:7524–7528.
21. **Frleta D, et al.** 2009. Influenza virus and poly(I:C) inhibit MHC class I-restricted presentation of cell-associated antigens derived from infected dead cells captured by human dendritic cells. J. Immunol. **182**: 2766–2776.
22. **Gentilini MV, Nunez GG, Roux ME, Venturiello SM.** 2011. Trichinella spiralis infection rapidly induces lung inflammatory response: the lung as the site of helminthocytotoxic activity. Immunobiology **216**:1054–1063.
23. **Gerlier D, Lyles DS.** 2011. Interplay between innate immunity and negative-strand RNA viruses: towards a rational model. Microbiol. Mol. Biol. Rev. **75**:468–490.
24. **Gilbert CR, Vipul K, Baram M.** 2010. Novel H1N1 influenza A viral infection complicated by alveolar hemorrhage. Respir. Care **55**:623–625.
25. **Giroux M, Schmidt M, Descoteaux A.** 2003. IFN-gamma-induced MHC class II expression: transactivation of class II transactivator promoter IV by IFN regulatory factor-1 is regulated by protein kinase C-alpha. J. Immunol. **171**:4187–4194.
26. **Goldman A, Bedolla G, Gebrail F, Cualing H.** 2003. Bronchus-associated lymphoid tissue lymphoma. Arch. Pathol. Lab. Med. **127**:115–116.
27. **Guarner J, Falcon-Escobedo R.** 2009. Comparison of the pathology caused by H1N1, H5N1, and H3N2 influenza viruses. Arch. Med. Res. **40**:655–661.
28. **Halle S, et al.** 2009. Induced bronchus-associated lymphoid tissue serves as a general priming site for T cells and is maintained by dendritic cells. J. Exp. Med. **206**:2593–2601.
29. **Hartshorn KL, White MR, Tecle T, Holmskov U, Crouch EC.** 2006. Innate defense against influenza A virus: activity of human neutrophil

defensins and interactions of defensins with surfactant protein D. J. Immunol. **176**:6962–6972.
30. **Hashimoto Y, Moki T, Takizawa T, Shiratsuchi A, Nakanishi Y.** 2007. Evidence for phagocytosis of influenza virus-infected, apoptotic cells by neutrophils and macrophages in mice. J. Immunol. **178**:2448–2457.
31. **Heier I, et al.** 2011. Characterisation of bronchus-associated lymphoid tissue and antigen-presenting cells in central airway mucosa of children. Thorax **66**:151–156.
32. **Helferty M, et al.** 2010. Incidence of hospital admissions and severe outcomes during the first and second waves of pandemic (H1N1) 2009. CMAJ **182**:1981–1987.
33. **Herberg JA, et al.** 2011. Comparison of pandemic and seasonal influenza reveals higher mortality and increased prevalence of shock in children with severe H1N1/09 infection. Pediatr. Infect. Dis. J. **30**:438–440.
34. **Hervas-Stubbs S, et al.** 2011. Direct effects of type I interferons on cells of the immune system. Clin. Cancer Res. **17**:2619–2627.
35. **Huang SS, et al.** 2011. Comparative analyses of pandemic H1N1 and seasonal H1N1, H3N2, and influenza B infections depict distinct clinical pictures in ferrets. PLoS One **6**:e27512. doi:10.1371/journal.pone.0027512.
36. **Itoh Y, et al.** 2009. In vitro and in vivo characterization of new swine-origin H1N1 influenza viruses. Nature **460**:1021–1025.
37. **Jain S, et al.** 2009. Hospitalized patients with 2009 H1N1 influenza in the United States, April-June 2009. N. Engl. J. Med. **361**:1935–1944.
38. **Jakeman KJ, Rushton DI, Smith H, Sweet C.** 1991. Exacerbation of bacterial toxicity to infant ferrets by influenza virus: possible role in sudden infant death syndrome. J. Infect. Dis. **163**:35–40.
39. **Jung K, et al.** 2010. Pathology in dogs with experimental canine H3N2 influenza virus infection. Res. Vet. Sci. **88**:523–527.
40. **Kelvin AA, et al.** 2012. Ferret TNF-α and IFN-γ immunoassays. *In* Abuelzein E (ed), Trends in immunolabelled and related techniques. InTech, Croatia.
41. **Kim B, et al.** 2011. Expression of myeloperoxidase in swine influenza virus (SIV)-infected neutrophils in lungs from pigs experimentally infected with SIV subtype H1N2. Vet. Res. Commun. **35**:469–475.
42. **Kumar A, et al.** 2009. Critically ill patients with 2009 influenza A(H1N1) infection in Canada. JAMA **302**:1872–1879.
43. **Libster R, et al.** 2010. Pediatric hospitalizations associated with 2009 pandemic influenza A (H1N1) in Argentina. N. Engl. J. Med. **362**:45–55.
44. **Lines JL, Hoskins S, Hollifield M, Cauley LS, Garvy BA.** 2010. The migration of T cells in response to influenza virus is altered in neonatal mice. J. Immunol. **185**:2980–2988.
45. **Louie JK, et al.** 2011. A review of adult mortality due to 2009 pandemic (H1N1) influenza A in California. PLoS One **6**:e18221. doi:10.1371/journal.pone.0018221.
46. **Luk J, Gross P, Thompson WW.** 2001. Observations on mortality during the 1918 influenza pandemic. Clin. Infect. Dis. **33**:1375–1378.
47. **Ma J, Dushoff J, Earn DJ.** 2011. Age-specific mortality risk from pandemic influenza. J. Theor. Biol. **288**:29–34.
48. **Maher JA, DeStefano J.** 2004. The ferret: an animal model to study influenza virus. Lab Anim. (NY) **33**:50–53.
49. **Maines TR, et al.** 2009. Transmission and pathogenesis of swine-origin 2009 A(H1N1) influenza viruses in ferrets and mice. Science **325**:484–487.
50. **Mamelund SE.** 2011. Geography may explain adult mortality from the 1918-20 influenza pandemic. Epidemics **3**:46–60.
51. **Marcelin G, et al.** 2011. Fatal outcome of pandemic H1N1 2009 influenza virus infection is associated with immunopathology and impaired lung repair, not enhanced viral burden, in pregnant mice. J. Virol. **85**:11208–11219.
52. **Martic J, et al.** 2011. Novel H1N1 influenza in neonates: from mild to fatal disease. J. Perinatol. **31**:446–448.
53. **Martina BE, et al.** 2003. Virology: SARS virus infection of cats and ferrets. Nature **425**:915. doi:10.1038/425915a.
54. **Martini M, et al.** 2010. IFN-gamma-mediated upmodulation of MHC class I expression activates tumor-specific immune response in a mouse model of prostate cancer. Vaccine **28**:3548–3557.
55. **Mauad T, et al.** 2010. Lung pathology in fatal novel human influenza A (H1N1) infection. Am. J. Respir. Crit. Care Med. **181**:72–79.
56. **Moyron-Quiroz JE, et al.** 2004. Role of inducible bronchus associated lymphoid tissue (iBALT) in respiratory immunity. Nat. Med. **10**:927–934.
57. **Munster VJ, et al.** 2009. Pathogenesis and transmission of swine-origin 2009 A(H1N1) influenza virus in ferrets. Science **325**:481–483.
58. **Nakajima N, et al.** 2012. Histopathological and immunohistochemical findings of 20 autopsy cases with 2009 H1N1 virus infection. Mod. Pathol. **25**:1–13.
59. **Narasaraju T, et al.** 2011. Excessive neutrophils and neutrophil extracellular traps contribute to acute lung injury of influenza pneumonitis. Am. J. Pathol. **179**:199–210.
60. **Okada T, et al.** 2011. Characteristic findings of pediatric inpatients with pandemic (H1N1) 2009 virus infection among severe and nonsevere illnesses. J. Infect. Chemother. **17**:238–245.
61. **O'Riordan S, et al.** 2010. Risk factors and outcomes among children admitted to hospital with pandemic H1N1 influenza. CMAJ **182**:39–44.
62. **Patterson AR, Cooper VL, Yoon KJ, Janke BH, Gauger PC.** 2009. Naturally occurring influenza infection in a ferret (Mustela putorius furo) colony. J. Vet. Diagn. Invest. **21**:527–530.
63. **Peltola VT, Boyd KL, McAuley JL, Rehg JE, McCullers JA.** 2006. Bacterial sinusitis and otitis media following influenza virus infection in ferrets. Infect. Immun. **74**:2562–2567.
64. **Perrone LA, Plowden JK, Garcia-Sastre A, Katz JM, Tumpey TM.** 2008. H5N1 and 1918 pandemic influenza virus infection results in early and excessive infiltration of macrophages and neutrophils in the lungs of mice. PLoS Pathog. **4**:e1000115. doi:10.1371/journal.ppat.1000115.
65. **Piazza FM, Carson JL, Hu SC, Leigh MW.** 1991. Attachment of influenza A virus to ferret tracheal epithelium at different maturational stages. Am. J. Respir. Cell Mol. Biol. **4**:82–87.
66. **Rangel-Moreno J, et al.** 2011. The development of inducible bronchus-associated lymphoid tissue depends on IL-17. Nat. Immunol. **12**:639–646.
67. **Rangel-Moreno J, et al.** 2006. Inducible bronchus-associated lymphoid tissue (iBALT) in patients with pulmonary complications of rheumatoid arthritis. J. Clin. Invest. **116**:3183–3194.
68. **Rangel-Moreno J, Moyron-Quiroz JE, Hartson L, Kusser K, Randall TD.** 2007. Pulmonary expression of CXC chemokine ligand 13, CC chemokine ligand 19, and CC chemokine ligand 21 is essential for local immunity to influenza. Proc. Natl. Acad. Sci. U. S. A. **104**:10577–10582.
69. **Renz H, Brandtzaeg P, Hornef M.** 2012. The impact of perinatal immune development on mucosal homeostasis and chronic inflammation. Nat. Rev. Immunol. **12**:9–23.
70. **Reuman PD, Keely S, Schiff GM.** 1989. Assessment of signs of influenza illness in the ferret model. J. Virol. Methods **24**:27–34.
71. **Rowe T, et al.** 2010. Modeling host responses in ferrets during A/California/07/2009 influenza infection. Virology **401**:257–265.
72. **Ruckwardt TJ, et al.** 2011. Neonatal CD8 T-cell hierarchy is distinct from adults and is influenced by intrinsic T cell properties in respiratory syncytial virus infected mice. PLoS Pathog. **7**:e1002377. doi:10.1371/journal.ppat.1002377.
73. **Saglanmak N, et al.** 2011. Gradual changes in the age distribution of excess deaths in the years following the 1918 influenza pandemic in Copenhagen: using epidemiological evidence to detect antigenic drift. Vaccine **29**(Suppl 2):B42–B48.
74. **Sarradell J, et al.** 2003. A morphologic and immunohistochemical study of the bronchus-associated lymphoid tissue of pigs naturally infected with Mycoplasma hyopneumoniae. Vet. Pathol. **40**:395–404.
75. **Schanzer D, Vachon J, Pelletier L.** 2011. Age-specific differences in influenza A epidemic curves: do children drive the spread of influenza epidemics? Am. J. Epidemiol. **174**:109–117.
76. **Seo SU, et al.** 2011. Type I interferon signaling regulates Ly6C(hi) monocytes and neutrophils during acute viral pneumonia in mice. PLoS Pathog. **7**:e1001304. doi:10.1371/journal.ppat.1001304.
77. **Shieh WJ, et al.** 2010. 2009 pandemic influenza A (H1N1): pathology and pathogenesis of 100 fatal cases in the United States. Am. J. Pathol. **177**:166–175.
78. **Shrestha SS, et al.** 2011. Estimating the burden of 2009 pandemic influenza A (H1N1) in the United States (April 2009-April 2010). Clin. Infect. Dis. **52**(Suppl 1):S75–S82.
79. **Simonsen L, et al.** 1998. Pandemic versus epidemic influenza mortality: a pattern of changing age distribution. J. Infect. Dis. **178**:53–60.
80. **Smith H, Sweet C.** 1988. Lessons for human influenza from pathogenicity studies with ferrets. Rev. Infect. Dis. **10**:56–75.
81. **Sugamata R, et al.** 2012. The contribution of neutrophil-derived myeloperoxidase in the early phase of fulminant acute respiratory distress syn-

drome induced by influenza virus infection. Microbiol. Immunol. **56**: 171–182.
82. **Sun CM, Deriaud E, Leclerc C, Lo-Man R.** 2005. Upon TLR9 signaling, CD5+ B cells control the IL-12-dependent Th1-priming capacity of neonatal DCs. Immunity **22**:467–477.
83. **Sun S, et al.** 2011. Age-related sensitivity and pathological differences in infections by 2009 pandemic influenza A (H1N1) virus. Virol. J. **8**:52.
84. **Sweet C, Jakeman KJ, Rushton DI, Smith H.** 1988. Role of upper respiratory tract infection in the deaths occurring in neonatal ferrets infected with influenza virus. Microb. Pathog. **5**:121–125.
85. **Tate MD, Brooks AG, Reading PC, Mintern JD.** 2012. Neutrophils sustain effective CD8(+) T-cell responses in the respiratory tract following influenza infection. Immunol. Cell Biol. **90**:197–205.
86. **Tate MD, et al.** 2009. Neutrophils ameliorate lung injury and the development of severe disease during influenza infection. J. Immunol. **183**: 7441–7450.
87. **Tate MD, et al.** 2011. The role of neutrophils during mild and severe influenza virus infections of mice. PLoS One **6**:e17618. doi:10.1371/journal.pone.0017618.
88. **Terai M, et al.** 2011. Early induction of interleukin-5 and peripheral eosinophilia in acute pneumonia in Japanese children infected by pandemic 2009 influenza A in the Tokyo area. Microbiol. Immunol. **55**:341–346.
89. **Thompson DL, et al.** 2011. Risk factors for 2009 pandemic influenza A (H1N1)-related hospitalization and death among racial/ethnic groups in New Mexico. Am. J. Public Health **101**:1776–1784.
90. **Thompson WW, et al.** 2004. Influenza-associated hospitalizations in the United States. JAMA **292**:1333–1340.
91. **Tschernig T, Pabst R.** 2000. Bronchus-associated lymphoid tissue (BALT) is not present in the normal adult lung but in different diseases. Pathobiology **68**:1–8.
92. **Tumpey TM, et al.** 2005. Pathogenicity of influenza viruses with genes from the 1918 pandemic virus: functional roles of alveolar macrophages and neutrophils in limiting virus replication and mortality in mice. J. Virol. **79**:14933–14944.
93. **Valtat S, Cori A, Carrat F, Valleron AJ.** 2011. Age distribution of cases and deaths during the 1889 influenza pandemic. Vaccine **29**(Suppl 2): B6–B10.
94. **van de Pavert SA, Mebius RE.** 2010. New insights into the development of lymphoid tissues. Nat. Rev. Immunol. **10**:664–674.
95. **Velilla PA, Rugeles MT, Chougnet CA.** 2006. Defective antigen-presenting cell function in human neonates. Clin. Immunol. **121**:251–259.
96. **Viboud C, Tam T, Fleming D, Miller MA, Simonsen L.** 2006. 1951 influenza epidemic, England and Wales, Canada, and the United States. Emerg. Infect. Dis. **12**:661–668.
97. **Wang G, et al.** 2010. "Default" generation of neonatal regulatory T cells. J. Immunol. **185**:71–78.
98. **Zenciroglu A, et al.** 2011. Swine influenza A (H1N1) virus infection in infants. Eur. J. Pediatr. **170**:333–338.
99. **Zhang AJ, et al.** 2011. High incidence of severe influenza among individuals over 50 years of age. Clin. Vaccine Immunol. **18**:1918–1924.
100. **Zhang X, et al.** 2007. Type I interferons protect neonates from acute inflammation through interleukin 10-producing B cells. J. Exp. Med. **204**:1107–1118.
101. **Zhang X, Yu S, Hoffmann K, Yu K, Forster R.** 2012. Neonatal lymph node stromal cells drive myelodendritic lineage cells into a distinct population of CX3CR1+CD11b+F4/80+ regulatory macrophages in mice. Blood **119**:3975–3986.